

Thermal transformation kinetics of a kaolinitic clay

A. D. Pekdemir¹ · Y. Sarıkaya² · M. Önal²

Received: 6 March 2015 / Accepted: 13 June 2015 / Published online: 11 July 2015
© Akadémiai Kiadó, Budapest, Hungary 2015

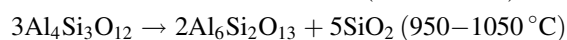
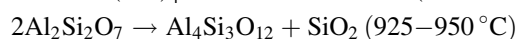
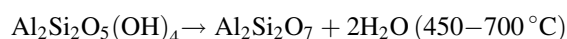
Abstract The objective of the present study was to use the zero-order reaction rate (ZORR) assumption and transition state theory (TST) to examine the kinetics of the thermal changes in solids. The method was firstly applied to the thermal transformation of spinel–mullite in a kaolinitic clay. The selected clay contains kaolinite (K), illite (I), and quartz (Q) minerals. The cylindrical compacts of the clay powder with a diameter of 40.22 mm were prepared under 150 MPa by uniaxial pressing using water (7 % by mass) as binder. The compacts after dried at 100 °C for 4 h were fired at various temperatures in the interval of 900–1050 °C by changing the time between 20 and 120 min. Besides the bulk density measurements, phase transformation in the compacts depending on the firing temperature was examined by X-ray diffraction and scanning electron microscopy techniques. Time derivative of the bulk densities for each firing temperature was taken as the transformation rate constant (k) according to the ZORR assumption. Arrhenius equation for the transformation was found as $k = A \exp(-E^\ddagger/RT) = (136 \text{ kg m}^{-3} \text{ s}^{-1}) \exp(-12,022 \text{ J mol}^{-1}/RT)$ where A is the preexponential factor, E^\ddagger is the activation energy, R is the universal gas constant and T is the absolute temperature of firing. The most general thermodynamic relation of the activation for the transformation was obtained from the TST with the SI units as $\Delta G^\ddagger = -RT \ln K^\ddagger = \Delta H^\ddagger - T\Delta S^\ddagger = 89,367 + 224T$ where ΔG^\ddagger , K^\ddagger , ΔH^\ddagger , and ΔS^\ddagger are the Gibbs energy, equilibrium constant, enthalpy,

and entropy for the activation of the thermal transformation, respectively. The positive value of the ΔG^\ddagger between 900 and 1050 °C indicated that the activation complex for the transformation does not form spontaneously.

Keywords Activation thermodynamics · Arrhenius equation · Density · Kaolinitic clay · Transformation kinetics · Transition state theory

Introduction

Thermal transformation in a compact is important for the ceramic production. Transformation kinetics is based on the measurement of any physical parameter depending on the time at different temperatures [1, 2]. Some of these parameters were arranged in rows as porosity, surface area, hardness, shrinkage, and density [3–8]. Several methods were reported in the literature for the determination of the kinetics parameters such as rate constant, activation energy, and preexponential factor as well as equilibrium constant, enthalpy, entropy, and Gibbs energy of the activation [9–14]. Since the kaolinitic clays (kaolins) are used as raw material in conventional porcelain production, their thermal behaviors have been extensively investigated [13, 15–17]. Major clay mineral of kaolins is called as kaolinite. Kaolinite is a hydroxylated aluminum silicate with an ideal structural formula $\text{Al}_2\text{Si}_2\text{O}_5(\text{OH})_4$. Chemical equation of thermal transformations for kaolinite mineral in the successive temperature intervals is reported as follows:



✉ M. Önal
onal@science.ankara.edu.tr

¹ Institute of Mineral Research and Exploration, Çankaya, 06800 Ankara, Turkey

² Department of Chemistry, Faculty of Science, University of Ankara, Tandoğan, 06100 Ankara, Turkey

where $\text{Al}_2\text{Si}_2\text{O}_7$ ($\text{Al}_2\text{O}_3 \cdot 2\text{SiO}_2$) is metakaolinite, $\text{Al}_4\text{Si}_3\text{O}_{12}$ ($2\text{Al}_2\text{O}_3 \cdot 3\text{SiO}_2$) is spinel, $2\text{Al}_6\text{Si}_2\text{O}_{13}$ ($3\text{Al}_2\text{O}_3 \cdot 2\text{SiO}_2$) is mullite and SiO_2 is an undistinguished silica [18–20].

The kinetics of spinel–mullite transformation in kaolinitic clays has not yet been examined as quantitatively. So, the aim of this study was to determine the kinetic parameters for this transformation by using bulk density measurements.

Experimental

Kaolinitic clay

Kaolinitic clay obtained from the Kalemaden Company, Turkey, was used as raw material. The clay was analyzed by X-ray fluorescence (XRF) technique. Thermogravimetric analysis (TG) and differential thermal analysis (DTA) curves were determined using a Thermoflex TG 8110 instrument. Approximately 20 mg of a sample was placed in a platinum crucible on the pan of the microbalance and heated in range 25–1000 °C using $\alpha\text{-Al}_2\text{O}_3$ as inert material. Analysis was performed under flowing nitrogen with the rate of 100 mL min^{-1} and at a heating rate of 10 °C min^{-1} . The Malvern Mastersizer 2000 instrument was used to obtain the particle size distribution (PSD) of the clay.

Compaction and firing

The clay powder was mixed with water (7 % by mass) and left overnight for homogeneous moisture dispersion. The samples taken from moisturized clay powder were compacted under 150 MPa by a uniaxial press (Toni Technik Baustoffprüfsysteme GmbH, Germany). The compacts having diameter 40.22 mm were dried in an oven at 100 °C for 4 h. They were fired to 900, 950, 1000, and 1050 °C with heating rate of 5 °C min^{-1} in a furnace (Protherm Model 130112, Alser, Turkey). Six different compacts were obtained at each temperature by taking the firing times as 20, 40, 60, 80, 100, 120 min.

Examination of the fired compacts

X-ray diffraction (XRD) patterns of the natural and fired compacts were recorded from the random mounts using a Rigaku Geigerflex D-MaxII TC Powder Diffractometer with a Ni filter and CuK_α ray with a wavelength of 0.15418 nm. Scanning electron microscopy (SEM) views for some fired compacts were recorded (Quanta 400 MK2) at 30 kV from samples that were after crashing covered with a gold thin film. The bulk density for each fired

compact was measured by mercury displacement technique at atmospheric pressure [21].

Results and discussion

Properties of the raw clay

The XRD pattern (Fig. 1) showed that the raw clay contains kaolinite (K), quartz (Q), and illite (I) minerals. K is a two-layered clay mineral, I a three-layered clay mineral, whereas Q is a crystalline silica.

The chemical analysis (CA) of the raw clay (in mass%) was determined as: SiO_2 , 57.75; Al_2O_3 , 25.85; Fe_2O_3 , 2.4; TiO_2 , 1.1; MgO , 0.8; CaO , 0.3; Na_2O , 0.4; K_2O , 2.4; and loss on ignition (LOI), 8.85. The SiO_2 is originated from the K, I, and Q minerals. The other oxides are due to K and I. The most possible source for the Fe_2O_3 and K_2O is the I mineral. The LOI is derived from the dehydroxylation of the K and I minerals. According to the ideal structural formula, molar ratio is $\text{Si}/\text{Al} = 1/1$ in kaolinite mineral. On the other hand, same ratio found by the chemical analysis is $\text{Si}/\text{Al} \cong 2/1$. The excess silicon is derived largely from the Q (SiO_2) and slightly from I minerals.

The TG and DTA curves of the raw clay (Fig. 2) showed consecutively endothermic and exothermic changes. The endothermic mass loss of 6.5 %, between 500 and 700 °C, with the maximum rate of change 570 °C, is due to the dehydroxylation of the K and I minerals. The exothermic change without mass loss between 950 and 1050 °C is

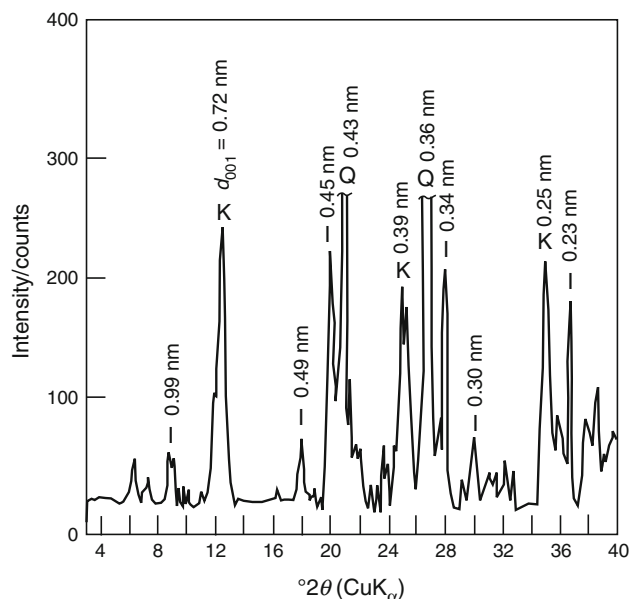


Fig. 1 XRD pattern of raw clay. I illite, K kaolinite, Q quartz

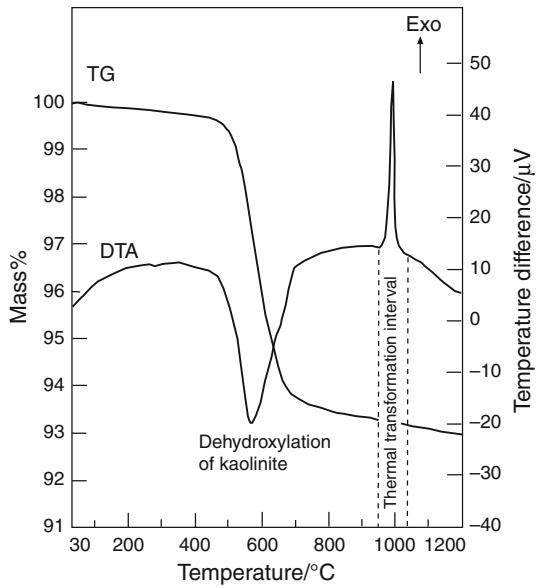


Fig. 2 DTA–TG analysis of raw clay

originated from the spinel–mullite transformation in the kaolinitic clay, which is the main subject of this study.

The particle size distribution (PSD) of the raw clay (Fig. 3) as volumetric percentage versus particle diameter (vol% vs. D) and its derivative $[d(\text{vol\%})/dD]$ vs. D indicated that the size of K, Q, and I particles changed between 1 and 100 μm , and mean particle size is around 8 μm .

Thermal transformation

The XRD patterns (Fig. 4) of the clay indicated that the crystal structures of K and I collapsed progressively before

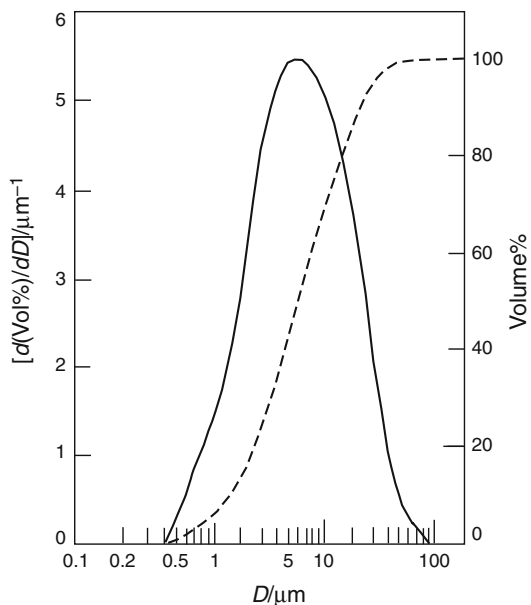


Fig. 3 PSD of the raw clay

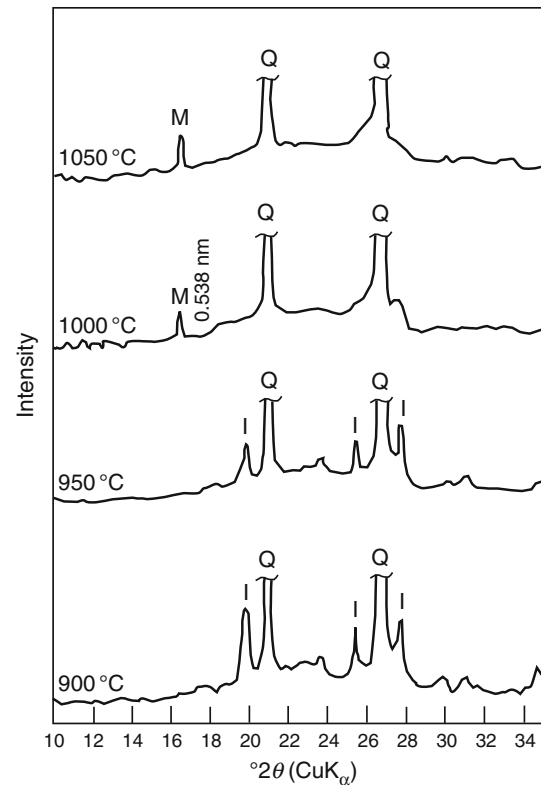


Fig. 4 XRD analysis of the heat treatment clays. *M* mullite, *Q* quartz, *I* illite

900 $^{\circ}\text{C}$ and after 950 $^{\circ}\text{C}$, respectively. Then, mullite is formed at 1000 $^{\circ}\text{C}$. Mullite content increased by the increase in firing temperature and fused with the quartz. The fusing of the solid particles is known as sintering. The size and volume of macropores with the radii greater than 100 nm decreased by the increase in the pelletizing pressure, whereas those of the nanopores decreased by the increase in the firing temperature [22].

The SEM views (Fig. 5) of two compacts before and after the thermal transformation indicated that the morphology and grain boundary of the particles in the compacts are changed by the progress in thermal transformation. The compact becomes so dense progressively, and sintering is completed. The increase in the density is due to the shrinkage of the compact by collapsing the nanopores during sintering [23].

The XRD, CA, TG/DTA, PSD, and SEM results revealed that the properties of the used raw material are similar compared to the raw kaolinitic clay reported in the literature.

Rate constant and Arrhenius equation

The plot of the bulk density versus time is a straight line with a high correlation for each firing temperature between

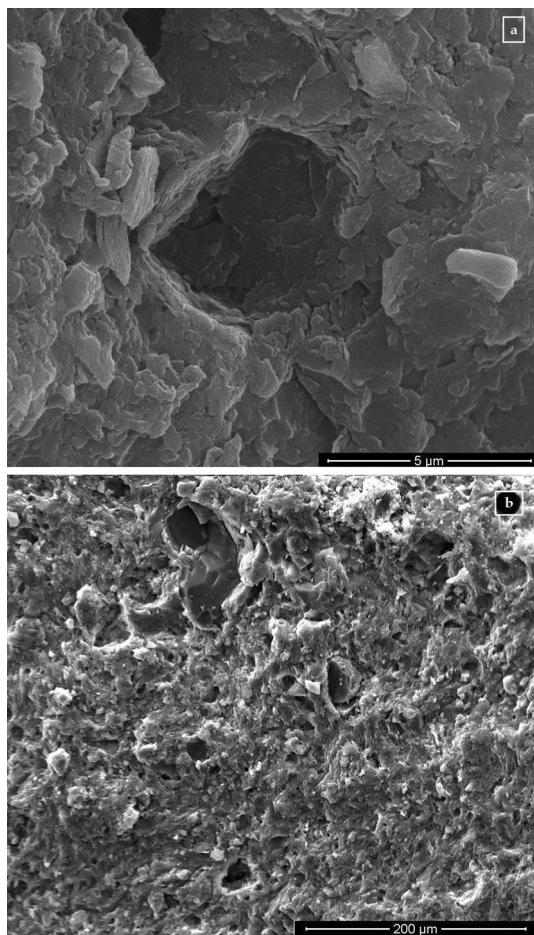


Fig. 5 SEM images of the sample of two heated temperatures. **a** 900 °C and **b** 1050 °C

900 and 1050 °C (Fig. 6). The equation of these straight lines can be written in the form given as below:

$$\rho = \rho_0 + kt \quad (1)$$

where t is time, ρ_0 is the density at $t = 0$ and k is rate constant assumed for thermal transformation of the kaolinite clay. This relation is similar to the zero-order reaction rate (ZORR) equation. Consequently, the rate constant was taken equal to the slope of the straight line with the units $\text{g cm}^{-3} \text{s}^{-1}$. The rate constants are given in Table 1 with the units $\text{kg m}^{-3} \text{s}^{-1}$.

The variation of logarithm of the rate constant ($\ln k$) with the reciprocal of the absolute firing temperature ($1/T$) found a straight line (Fig. 7). The straight line obeys to Arrhenius equation written in the form as below:

$$\ln k = -\frac{E^\#}{RT} + \ln A \quad (2)$$

where $E^\#$ is activation energy, A is frequency factor, $R = 8.314 \text{ J mol}^{-1} \text{ K}^{-1}$ is the universal gas constant and T is the absolute firing temperature. The Arrhenius parameters

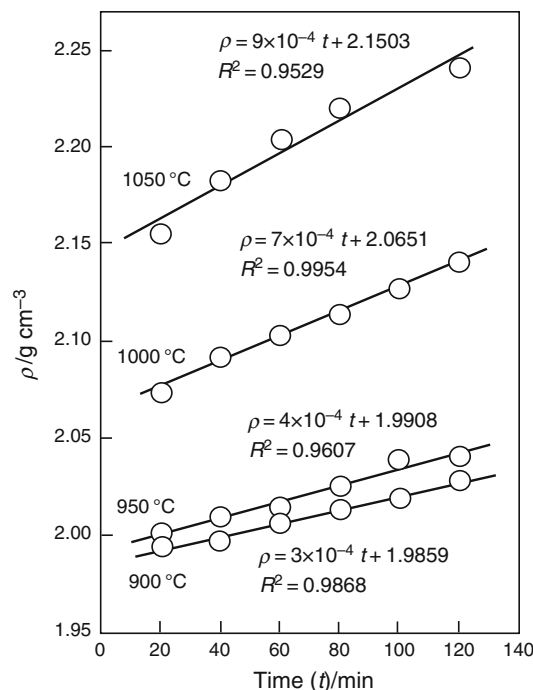


Fig. 6 Straight lines of the density as a function of time for four firing temperatures

were calculated from slope and intercept of the straight line as $E^\# = 99,951 \text{ J mol}^{-1}$ and $A = 136 \text{ kg m}^{-3} \text{ s}^{-1}$. Hence, temperature dependence of the rate constant is express as:

$$k = (136 \text{ kg m}^{-3} \text{ s}^{-1}) \times \exp(-99,951 \text{ J mol}^{-1}/RT) \quad (3)$$

This relation is valid only for the thermal transformation of spinel to mullite at temperatures between 900 and 1050 °C.

Thermodynamic parameters of activation

According to the transition state theory (TST), reactants in a reaction are in equilibrium with an unstable activated complex (AC) and all thermodynamic relations are valid for this equilibrium. Relation between rate constant (k) and equilibrium constant ($K^\#$) for the formation of an AC can be given in Eyring equation derived from the TST [24, 25]:

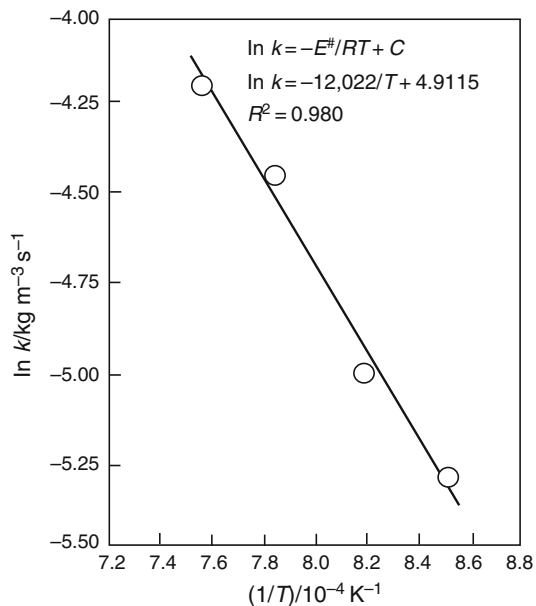
$$K^\# = \frac{kh}{k_B T} \quad (4)$$

where $k_B = 1.38 \times 10^{-23} \text{ J K}^{-1}$ is the Boltzmann constant, $h = 6.62 \times 10^{-34} \text{ J s}$ is the Planck constant and T is the absolute temperature. The $K^\#$ value for each firing temperature was calculated from Eyring equation given in Table 1.

The variation of logarithm of the equilibrium constant ($\ln K^\#$) with the reciprocal of the absolute firing temperature ($1/T$) found a straight line as seen in Fig. 8. The straight line obeys to van't Hoff equation written in the form as below:

Table 1 Kinetic parameters for the thermal transformation of kaolinitic clay (t , T firing temperature, k rate constant, $K^\#$ equilibrium constant of activation)

$t/^\circ\text{C}$	T/K	$(1/T)/10^{-4} \text{ K}^{-1}$	$k/10^{-3} \text{ kg m}^{-3} \text{ s}^{-1}$	$\ln k$	$K^\#/10^{-16} \text{ m}^3 \text{ mol}^{-1}$	$\ln K^\#$
900	1173	8.52	5.00	-5.30	2.05	-36.12
950	1223	8.18	6.67	-5.01	2.62	-35.88
1000	1273	7.85	11.67	-4.45	4.40	-35.36
1050	1323	7.56	15.00	-4.20	5.44	-35.15

**Fig. 7** Arrhenius plot for sintering of the clay

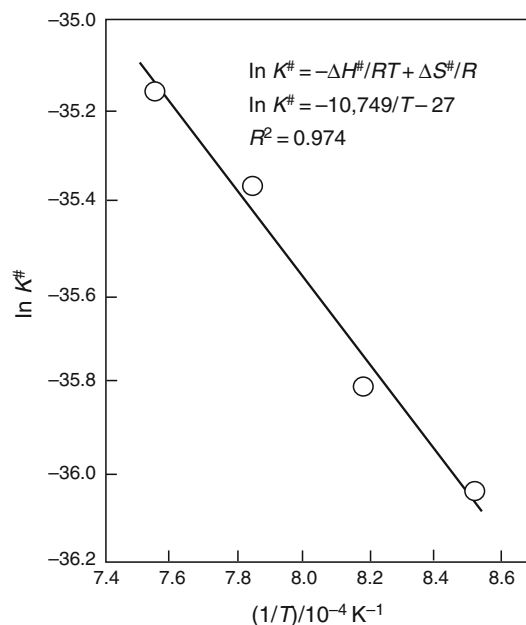
$$\ln K^\# = -\frac{\Delta H^\#}{RT} + \frac{\Delta S^\#}{R} \quad (5)$$

where $\Delta H^\#$ and $\Delta S^\#$ are the enthalpy and entropy of the activation, respectively. These thermodynamic parameters were calculated from slope and intercept of the straight line as $\Delta H^\# = 89,367 \text{ J mol}^{-1}$ and $\Delta S^\# = -224 \text{ J mol}^{-1} \text{ K}^{-1}$. These values indicated that the formation of the activated complex is endothermic and takes place a decrease in disorder. Inversely, the decomposition of the activated complex is exothermic as seen in Fig. 2.

According to the basic thermodynamic equation, a relationship between the thermodynamic parameters for the activation can be written as below:

$$\Delta G^\# = -RT \ln K^\# = \Delta H^\# - T\Delta S^\# = 89,367 + 224T \quad (6)$$

where $\Delta G^\#$ is the free enthalpy (Gibbs energy) of the activation. The increase in $\Delta G^\#$ at temperatures between 900 and 1050 $^\circ\text{C}$ indicates that the chemical equilibrium of transition state does not form spontaneously.

**Fig. 8** Straight lines of the equilibrium constant as a function of firing temperature

Conclusions

The various physicochemical changes in solids such as dehydration, dehydroxylation, calcinations, decomposition, crystal transformation, and sintering can be examined kinetically as similar in this study. The measurable kinetic variables depending on both the time and temperature can be selected to be density, shrinkage, porosity, surface area, hardness, crystallinity, etc. The rate constant and its temperature dependence can be evaluated from the zero-order reaction rate assumption and Arrhenius equation, respectively. In order to obtain equilibrium constant, enthalpy, entropy, and free enthalpy of thermal activation, the transition state theory could be used.

Acknowledgements The authors thank to Ankara University Research Fund (Project No.: 12B4240016) for financial support to this work.

References

1. Kingery WD, Bowen HK, Uhlmann DR. Introduction to ceramics. 2nd ed. New York: Wiley-Interscience; 1976.
2. Kang SJL. Sintering densification grain growth and microstructure. Butterworth: Elsevier; 2005.
3. German RM. Sintering theory and practice. New York: Wiley; 1996.
4. Bartholomew CH. Sintering kinetics of supported metals: new perspectives from a unifying GPLE treatment. *Appl Catal A Gen.* 1993;107:1–57.
5. Su H, Johnson DL. Practical approach to sintering. *Am Ceram Soc Bull.* 1997;76:72–6.
6. Perez-Maqueda LA, Criado JM, Real C. Kinetics of the initial stage of sintering from shrinkage data: simultaneous determination of activation energy and kinetic model from a single non-isothermal experiment. *J Am Ceram Soc.* 2002;85:763–8.
7. Roy SN, Saha SR, Guha SK. Sintering kinetics of pure and doped chromium oxide. *J Mater Sci.* 1986;21:3673–6.
8. Thompson AM, Harmer MP. Influence of atmosphere on the final-stage sintering kinetics of ultra-high-purity alumina. *J Am Ceram Soc.* 1993;76:2248–56.
9. Ting CJ, Lu HY. Defect reactions and the controlling mechanism in the sintering of magnesium aluminate spinel. *J Am Ceram Soc.* 1999;82:841–8.
10. Wang H, Liu X, Chen F, Meng G, Sorensen OT. Kinetics and mechanism of a sintering process for macroporous alumina ceramics by extrusion. *J Am Ceram Soc.* 1998;81:781–4.
11. German RM, Munir ZA. Surface area reduction during isothermal sintering. *J Am Ceram Soc.* 1976;59:379–83.
12. Sarıkaya Y, Ada K, Önal M. Applications of the zero-order reaction rate model and transition state theory on the intra-particle sintering of an alumina powder by using surface area measurements. *J Alloy Compd.* 2007;432:194–9.
13. Wang H, Li C, Peng Z, Zhang S. Characterization and thermal behavior of kaolin. *J Therm Anal Calorim.* 2011;105:157–60.
14. Wang Z, Marin G, Naterer GF, Gabriel KS. Thermodynamics and kinetics of the thermal decomposition of cupric chloride in its hydrolysis reaction. *J Therm Anal Calorim.* 2015;119:815–23.
15. Dion P, Alcover JF, Bergaya F, Ortega A, Llevellyn PL, Rouquerol F. Kinetic study by controlled-transformation rate thermal analysis of the dehydroxylation of kaolinite. *Clay Miner.* 1998;33:269–76.
16. Edomwonyi-Otu LC, Aderemi BO, Ahmed AS, Coville NJ, Maaza M. Influence of thermal treatment on Kankara kaolinite. *Opticon.* 1826;2013(15):1–5.
17. Chakraborty AK. Phase transformation of kaolinite clay. Berlin: Springer; 2014.
18. Kahraman S, Önal M, Sarıkaya Y, Bozdoğan İ. Characterization of silica polymorphs in kaolins by X-ray diffraction before and after phosphoric acid digestion and thermal treatment. *Anal Chim Acta.* 2005;552:201–6.
19. Önal M, Sarıkaya Y. The effect of heat treatment on the paracrystallinity of an opal-CT found in a bentonite. *J Non-Cryst Solids.* 2007;353:4195–8.
20. Önal M, Kahraman S, Sarıkaya Y. Differentiation of α -cristobalite from opals in bentonites from Turkey. *Appl Clay Sci.* 2007;35:25–30.
21. Choudhary VR, Vaidya SH. Simple specific gravity bottle methods for measuring porosity of solid catalysts and adsorbents. *Res Ind.* 1981;26:1–3.
22. Hugo P, Koch H. Production of porous alumina with defined bimodal pore structure. *Ger Chem Eng.* 1979;2:24–30.
23. Baran B, Sarıkaya Y, Alemdaroğlu T, Önal M. The effect of boron containing frits on the anorthite formation temperature in kaolin-wollastonite mixtures. *J Euro Ceram Soc.* 2003;21:2061–6.
24. Ada K, Önal M, Sarıkaya Y. Investigation of the intra-particle sintering kinetics of a mainly agglomerated alumina powder by using surface area reduction. *Powder Technol.* 2006;168:37–41.
25. Sarıkaya Y, Önal M. High temperature carburizing of a stainless steel with uranium carbide. *J Alloys Compd.* 2012;542:253–6.